https://doi.org/10.5194/egusphere-2026-4471
Preprint. Discussion started: 4 August 2026

Updating Thermal Head of Recoverable Autonomous Sonde (RECAS) for Better Drilling Performance in Qilin Subglacial Lake Exploration

Yazhou Li[1,2], Xuxin Lei[1,2], Xiaopeng Fan[3], Haibing Yu[4], Bing Li[1,2], Shilin Peng[4], Yuting Ye[1,2]

[1]State Key Laboratory of Deep Earth Exploration and Imaging, School of Engineering and Technology, China University of Geosciences, Beijing, 100083, China

[2]Key Laboratory of Polar Geology and Marine Mineral Resources (China University of Geosciences, Beijing), Ministry of Education, Beijing, 100083, China

[3]Institute of Polar Science and Engineering, College of Construction Engineering, Jilin University, Changchun, 130021, China

[4]College of Electronics and Information, Hangzhou Dianzi University, Hangzhou, 310018, China

Corresponding to: Xiaopeng Fan (fxp@jlu.edu.cn)

Abstract. There are numerous subglacial lakes in Antarctica, typically covered by thick ice sheets. Qilin subglacial lake is one of the largest subglacial lakes in Antarctica, lying beneath approximately 3600 m of ice. The exploration of this unique environment is of considerable scientific importance. Recoverable Autonomous Sonde (RECAS) has been proposed for exploring Qilin subglacial lake. However, drilling into the lakes with such probe may be impeded by volcanic ash or small rock clasts within the ice sheet. In addition, RECAS is incapable of withstanding the extreme hydrostatic pressure existing in the Qilin subglacial lake. To address these challenges, the thermal head of RECAS was redesigned and fabricated. Compared with the original RECAS thermal head, the updated thermal head has extra water circulation unit. Laboratory test validated that the redesigned RECAS thermal head can operate at water pressures of up to 40 MPa. Moreover, its rate of penetration (ROP) improved by 21.1 % in clean ice, by 41.1 % in dust-laden ice, and by 253.4 % in ice with debris-rich ice. The updated RECAS thermal head is expected to be utilized to drill Qilin Subglacial Lake in the coming Antarctic work season.

https://doi.org/10.5194/egusphere-2026-4471
Preprint. Discussion started: 4 August 2026

1 Introduction

Glaciers, ice caps, ice sheets and permafrost are widely distributed in the polar regions of the Earth (Tsytovich, 1975; Cuffey and Paterson, 2010; Kutasov and Eppelbaum, 2018; Eppelbaum and Kutasov, 2019), Antarctica, located in the southernmost part of the Earth, is largely covered by massive ice sheets (Fretwell et al., 2013). In the 1970s, the presence of subglacial liquid water in Antarctica was first discovered (Robin et al., 1970; Oswald and Robin, 1973). With continuous international exploration, hundreds of subglacial lakes have been identified in Antarctica (Livingstone et al., 2022). Antarctic subglacial lakes preserve key information regarding ice sheet dynamics and paleoclimatic changes, serving as natural platforms for exploring extremophilic life, the deep biosphere, and extraterrestrial habitability (Priscu et al., 1999; Siegert, 2000; Christner et al., 2014).

In recent years, a large Subglacial Lake named Qilin has been discovered by geophysical surveys in Princess Elizabeth Land, East Antarctica (Fig. 1). This lake is covered by approximately 3600-m-thick ice sheet, has been isolated from the surface for millions of years, and exhibits unique morphological and sedimentary characteristics (Yan et al., 2022, 2025; Li et al., 2026; Lu and Chen, 2026). Further investigation of Qilin Subglacial Lake and the advancement of deep-drilling technologies will promote interdisciplinary polar research.

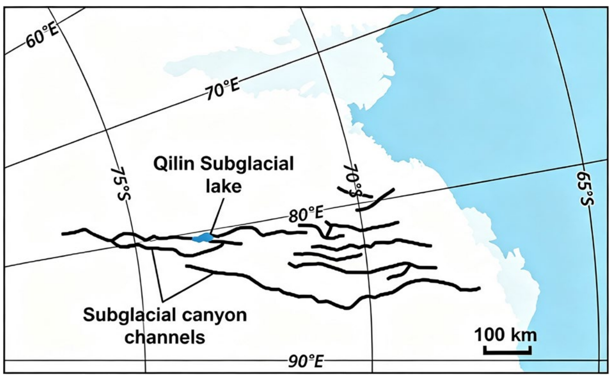

Figure 1. Location of the Qilin subglacial lake in Antarctica (Yan et al., 2022, modified)

Subglacial lake drilling methods can be divided into mechanical drilling and thermal drilling. The mechanical drilling conducted by Russia at Subglacial Lake Vostok is a typical early example. Although this method obtained subglacial lake

https://doi.org/10.5194/egusphere-2026-4471
Preprint. Discussion started: 4 August 2026

water samples for the first time, the use of hydrocarbon drilling fluids inevitably introduced chemical and biological contamination, significantly reducing the scientific value of the recovered samples (Bulat, 2016). To achieve clean sampling, the focus of global research has gradually shifted toward thermal drilling technologies. In December 2012, a British team attempted to explore Subglacial Lake Ellsworth using a clean hot-water drilling system; however, the effort did not succeed (Siegert et al., 2012, 2014). In January 2013, the U.S. Whillans Ice Stream Subglacial Access Research Drilling (WISSARD) project employed filtered and sterilized hot-water drilling technology, successfully collecting uncontaminated samples and directly confirming the existence of subglacial microorganisms (Christner et al., 2014). In December 2018, the U.S. Subglacial Antarctic Lakes Scientific Access (SALSA) team adopted a hot-water drilling system similar to that used in the WISSARD project and successfully obtained water and sediment samples from Subglacial Lake Mercer (Priscu et al., 2021).

Thermal melt probes, which use electrically heated thermal heads to melt through ice, are considered one of the cleanest drilling tools for exploring subglacial lakes and similar aquatic environments under subglacial oceans on extraterrestrial planets. Accordingly, several thermal melt probes, such as IceMole, IceShuttle Teredo, TRIPLE, have been designed (Dachwald et al., 2014; Wirtz and Hildebrandt, 2016; Heinen et al., 2021). RECAS is a recoverable thermal melt probe designed for both downward and upward drilling and has been proposed for exploring Qilin subglacial lake (Talalay et al., 2014; Zhou et al., 2024). Field tests in Antarctica have demonstrated that RECAS prototype operates reliably (Sun et al., 2024). However, RECAS was designed only for drilling in clean ice. In practice, ice sheets usually have dusty ice layers, which typically contain volcano ash (Narcisi et al., 2017; Kohno et al., 2004). For example, twenty-six ash layers with thickness varying 1–24 mm were found in a 2503m deep ice core from Dome Fuji station (Kohno et al., 2004). Moreover, rock clasts are often present at the base of the ice sheet overlying the subglacial lake, which can similarly impede the penetration of thermal melt probe (Leitchenkov et al., 2007, 2016).

Domestic tests of the RECAS prototype indicate that solid particles, such as dust and sand, tend to accumulate on the thermal head during drilling in dusty ice, thereby impeding heat transfer and reducing the ROP. The existing dust collection device, mounted above RECAS lower thermal head, can only mitigate particle deposition rather than fundamentally solving this limitation, resulting in a persistent discrepancy between the actual and expected ROPs (Li et al., 2020). Additionally, the

https://doi.org/10.5194/egusphere-2026-4471
Preprint. Discussion started: 4 August 2026

hydrostatic pressure imposed by the overlying ice sheet on Qilin subglacial lake is approximately 36 MPa, which exceeds the pressure tolerance of the existing RECAS thermal head (Li et al., 2020). In conclusion, the existing RECAS thermal melt probe is insufficient to fulfill the exploration needs of Qilin subglacial lake.

Hot-water drills with downhole self-circulation (HWDDSC) can heat and circulate meltwater in situ at the borehole bottom Characterized by a high ROP and contamination-free operations, HWDDSC can provide critical technical support for efficient drilling in ice containing dust or solid rock clasts. Since the first HWDDSC was developed in 1972, a wide range of such drilling systems have been developed and deployed globally (Gillet, 1975; Hantz and Lliboutry, 1983). The Cryobot, initially conceived in 1998, combined electric heating with a hot-water jet system to improve cleaning and drilling efficiency in polar and extraterrestrial ice environments (Zimmerman et al., 2001, 2002). Recent developments in melt probe combining hot-water jetting, including VALKYRIE and SPINDLE, have demonstrated the feasibility of combining thermal melting and bidirectional hot-water jetting to improve penetration performance and operational robustness in debris-rich ice environments (Stone et al., 2014, 2018). A drilling system with near-bottom hot water circulation was developed in Jilin University, and it can remove fine dust from borehole bottom by meltwater jetting, thereby improving drilling performance in ice containing dust (Zhao et al., 2022). However, its low-pressure tolerance precludes it from meeting the stringent pressure requirements of Qilin subglacial lake exploration. Additionally, technologies to make thermal head melting curvilinearly was also developed to avoid rock clasts (Schüller et al., 2016; Sysoev et al., 2025). However, this technology requires precise advance detection of rock clasts and involves rather complex operations.

In this study, the RECAS thermal head was redesigned by introducing extra water-jetting component and filtration component. Then, the hydrostatic pressure test and drilling test in clear ice, in dust-laden ice and in debris-rich ice were conducted to evaluate the performance of the updated RECAS thermal head.

https://doi.org/10.5194/egusphere-2026-4471
Preprint. Discussion started: 4 August 2026

2 General concept

2.1 Technical requirements

To successfully penetrate the ice sheet and access Qilin Subglacial Lake, the improved RECAS thermal probe must withstand a hydrostatic pressure of no less than 36 MPa. Therefore, its rated pressure is set to 40 MPa to ensure an adequate safety margin. In addition, to achieve efficient drilling and sampling, the target ROP is required to exceed 2 m h^{-1}. The thermal probe is designed to match the outer diameter of the RECAS drilling system, which is 180 mm. In order to be compatible with the entire RECAS system, the new thermal head is required to operate at a voltage of no less than 650 V during heating.

The probe is expected to operate stably under various ice conditions, including clean ice, dust-bearing ice, and debris-rich ice, while maintaining a relatively constant ROP. This ensures continuous and reliable drilling performance and significantly improves the capability for subglacial lake exploration and sampling. The overall technical specifications of the improved RECAS thermal probe are summarized in Table 1.

Table 1. Technical requirements of the updated RECAS thermal head

Aspects	Requirements
Diameter	180 mm
ROP	>2 m h^{-1}
hydrostatic pressure resistance	≥40 MPa
Working voltage	650 V
Drilling capacity	Clean ice Dust-laden ice Debris-rich ice

https://doi.org/10.5194/egusphere-2026-4471
Preprint. Discussion started: 4 August 2026

2.2 Conceptual model

Based on the technical requirement and the previous research foundation of the RECAS thermal head, an updated design that integrates thermal melting drilling with downhole meltwater self-circulation was proposed to achieve better drilling performance in Qilin subglacial lake exploration. As shown in Fig. 2, the updated RECAS thermal head still uses cartridge heaters inserted into its body to generate heat for melting ice, and a pressure housing above the thermal head protects the cartridge heaters from high water pressure. A pump is installed above the pressure housing to generate water flow near the bottom of the borehole. To protect the pump from damaged by solid particles in the borehole, a filter should be installed at the pump inlet. When the pump starts, water is drawn from the annulus between the RECAS thermal head and the borehole wall, conveyed along a water channel at the center of the thermal head, and finally jetted out through a nozzle at the tip of the thermal head body. If dust particles are deposited at the bottom of the borehole, the water jet from the nozzle is expected to wash them away from the bottom and collect them in the internal cavity of the thermal head. The filter allows only water to pass through while blocking solid particles.

When drilling in clean ice, the pump is not usually used; melting relies solely on the heat generated by the cartridge heaters. Of course, the pump can also be operated during clean ice drilling to enhance heat transfer between the thermal head and the surrounding ice. When drilling in dust-laden ice, the pump must be started. In this way, the adverse effects of impurities on the heat transfer of the thermal head can be mitigated, thereby optimizing heat distribution and energy utilization, and ultimately enhancing drilling performance in complex ice conditions.

https://doi.org/10.5194/egusphere-2026-4471
Preprint. Discussion started: 4 August 2026

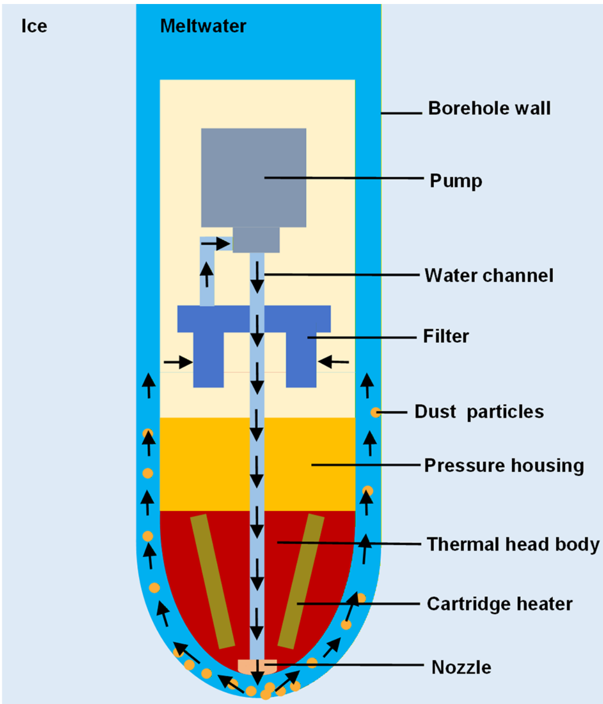

Figure 2. Schematic diagram of the updated RECAS thermal head

3 Design of the updated RECAS thermal head

3.1 Calculation of power consumption

In this study, the empirical formula from previous research was adopted to quantitatively calculate the heating power of the thermal head as a function of the ROP (Li et al., 2020). In the calculations, the thermal head diameter was set as 180 mm, and three typical ROPs of 2 m/h, 2.5 m/h and 3 m/h were selected as operating conditions. and the thermal drilling efficiency was assumed to be 85 %. Based on estimated ice temperature from the overlying 500 m ice sheet above Qilin Subglacial Lake, the ice temperature was determined to be >−16 °C (Li et al., 2026). The calculated power consumption for the different conditions is presented in Fig. 3.

https://doi.org/10.5194/egusphere-2026-4471
Preprint. Discussion started: 4 August 2026

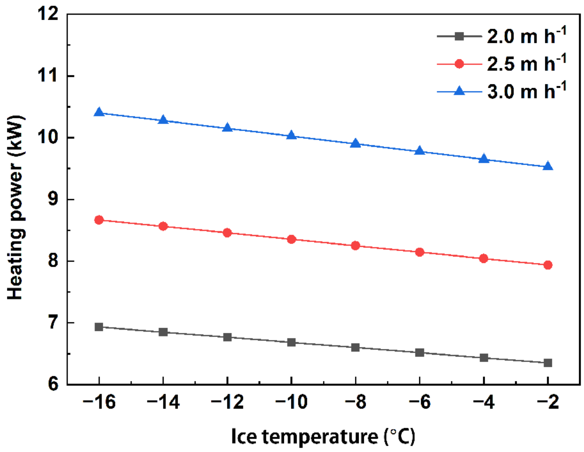

Figure 3. Calculation of power consumption

The results indicate that the required heating power has a significant negative correlation with ice temperature; that is, a higher ice temperature corresponds to a lower heating power. The temperature of the upper ice sheet in the drilling site reaches its minimum of approximately −16 °C, resulting in the maximum heating power demand. Under this low-temperature condition, the required heating power is 6.9 kW at a ROP of 2 m h^{-1} and rises to 10.4 kW when the rate increases to 3 m h^{-1}. Taking into account long-term stable operation and a sufficient safety margin, the rated heating power of the thermal head was ultimately determined to be 7 kW for required ROPs above 2 m h^{-1}.

3.2 Determination of pump flow rate

The flow rate of the pump is a critical design parameter, as it determines the water velocity in the borehole and, in turn, whether dust particles can be flushed out of the bottom. The following presents numerical and experimental methods used to determine the pump flow rate.

3.2.1. Numerical investigation

During dust particles movement, the actual velocity of dust particles is the vector sum of water flow velocity v_a and particle settling velocity v_t. The annular flow inside the gap between thermal head and borehole wall is generally upward, which is

https://doi.org/10.5194/egusphere-2026-4471
Preprint. Discussion started: 4 August 2026

mainly controlled by the flow rate of the built-in pump. Dust particles in the borehole exhibit three motion modes: rising, suspension and settling. Settling particles driven by gravity tend to accumulate at the thermal head tip, impeding heat transfer and reducing thermal efficiency. Based on the principle of velocity superposition, the vertical upward direction is taken as positive, with $v_a > 0$ and $v_t < 0$. The motion state of a particle is determined by the resultant velocity: it rises when $v_a+v_t > 0$, remains suspended when $v_a+v_t = 0$, and settles when $v_a+v_t < 0$. Therefore, the minimum water velocity should be bigger than the setting velocity of particles, namely, $v_a>-v_t$. Consequently, the minimum flow rate to prevent solid particles accumulate at borehole bottom can be calculated by following expression

$$Q=-A_a v_t \quad (1)$$

$$A_a=\frac{\pi}{4}(D^2-d^2) \quad (2)$$

Where Q is the fluid flow rate passing through the annulus, m^3 s^{-1}; A_a is the area of the annulus cross section between thermal head and ice borehole wall, m^2; D and d are borehole diameter and thermal head diameter, respectively, m.

In this study, a numerical model was developed in COMSOL Multiphysics 6.1 software to calculate the particle settling velocity. In the model, the steady settling velocity is obtained by simulating the motion of a single dust particle in the annular flow field. Considering the axisymmetric characteristic of the annulus and the dust particle, the three-dimensional model can be simplified to a two-dimensional one, which effectively reduces the computational complexity. The simplified two-dimensional physical model for simulating setting velocity of single dust particle is shown in Fig. 4. In the model, the water is assumed to flow upward at a gradually increasing velocity until the dust particle can remain stably suspended.

https://doi.org/10.5194/egusphere-2026-4471
Preprint. Discussion started: 4 August 2026

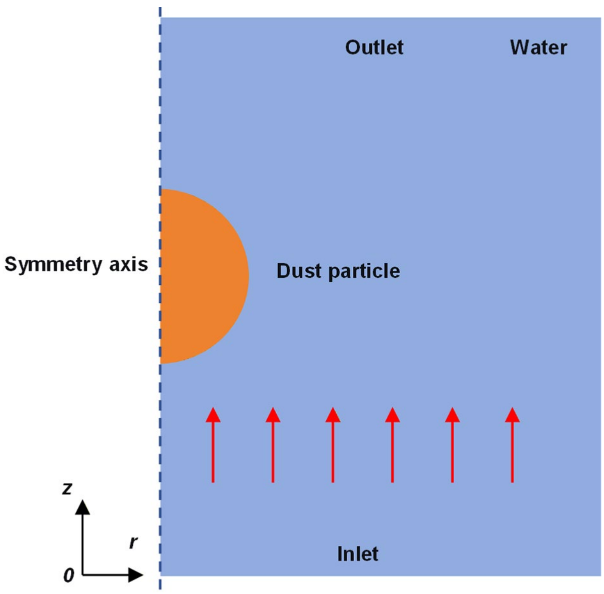

Figure 4. Physical model for simulating setting velocity of single dust particles

This numerical model is based on fluid mechanics theory. The Navier–Stokes equation can be used to describe water flow

$$\rho\frac{\partial \boldsymbol{u}}{\partial t}-\nabla\cdot\mu(\nabla\boldsymbol{u}+(\nabla\boldsymbol{u})^{T})+\rho\boldsymbol{u}\cdot\nabla\boldsymbol{u}+\nabla p=\boldsymbol{F} \tag{3}$$

$$\nabla\cdot\boldsymbol{u}=0 \tag{4}$$

where ρ is the water density, 1000 kg m^{-3}, $\boldsymbol{u}$ is the water velocity, m s^{-1}; μ is the water viscosity, 1.51×10^{-3} N s m^{-2}; and p is the fluid pressure, Pa. $\boldsymbol{F}$ is volume force density and can be expressed as

$$F_r=0 \tag{5}$$

$$F_z=-\rho(a+g) \tag{6}$$

where a is the acceleration of dust particles, m s^{-2}; and g is the gravitational acceleration, 9.81 m s^{-2}.

The force balance equation of dust particles adopts an ordinary differential equation

$$mx=F_g+F_z \tag{7}$$

where m is the mass of dust particles, kg; x represents the particle position, m; F_g is the gravitational force, and F_z is the z-component of the force that the water exerts on particles. The expression of gravitational force is given as follows

https://doi.org/10.5194/egusphere-2026-4471
Preprint. Discussion started: 4 August 2026

$$F_g = -\rho_g V_g g \quad (8)$$

where V_g is the volume of dust particles, m^3; and ρ_g is the particle density, 2600 kg m^{-3}.

The force that the water exerts on the grain could be calculated by integrating the normal component of the stress tensor over the surface of the particle.

$$F_z = 2\pi \int_S r\dot{\boldsymbol{z}} \cdot [-pI + \mu(\nabla \boldsymbol{u} + (\nabla \boldsymbol{u})^T)]\boldsymbol{n} dS \quad (9)$$

where r is the radial coordinate, $\dot{\boldsymbol{z}}$ is the unit vector in the z-direction, and $\boldsymbol{n}$ denotes the normal vector on the dust particle surface.

The initial values for position and velocities are

$$u_0 = v_0 = x_0 = \frac{dx_0}{dt} = 0 \quad (10)$$

At the particle's surface, the water velocity relative to the particle is zero, that is

$$\boldsymbol{u} = 0 \quad (11)$$

At the inlet of the water domain the velocity equals the falling velocity:

$$\boldsymbol{u} = (0, \frac{dx}{dt}) \quad (12)$$

Furthermore, a neutral condition describes the outlet, which is

$$\mathbf{n} \cdot [-pI + \mu(\nabla \boldsymbol{u} + (\nabla \boldsymbol{u})^T)] = 0 \quad (13)$$

The aforementioned equations can be numerically solved in COMSOL Multiphysics 6.1 software. As an example, Fig. 5 illustrates the time-dependent settling velocity of 100-μm particles obtained from simulations. The velocity stabilizes at approximately 0.015 s, and this steady value (0.045 m s^{-1}) is defined as the terminal settling velocity for 100-μm dust particle.

https://doi.org/10.5194/egusphere-2026-4471
Preprint. Discussion started: 4 August 2026

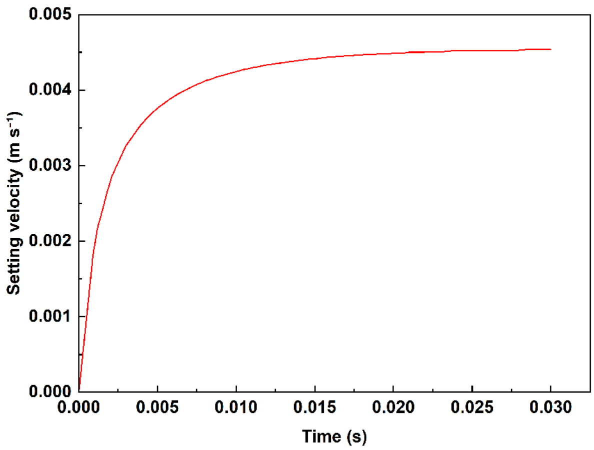

Figure 5. Temporal evolution of simulated settling velocity for 100-μm particles

The settling velocities of dust particles with diameters from 10 μm to 300 μm were calculated from simulations, with results presented in Fig. 6. For particle sizes below 75 μm, the settling velocity increases slowly with increasing diameter; beyond this threshold, the velocity rises almost linearly with size, reaching 0.0325 m s^{-1} at 300 μm. In Antarctica ice sheet, the size of dust particles is usually less than 100 μm. Therefore, a water velocity of 0.0054 m·s^{-1} is enough to suspend the dust particle. Based on previous experience with the RECAS thermal head, the borehole diameter in dirty ice is typically 20–25 mm larger than that of the thermal head (Li et al., 2020). Therefore, it is reasonable to assume that the updated RECAS thermal head will produce a borehole 200–205 mm in diameter. Using equations (1) and (2), the minimum pump flow rate is estimated to be 1.93−2.44 L min^{-1}.

https://doi.org/10.5194/egusphere-2026-4471
Preprint. Discussion started: 4 August 2026

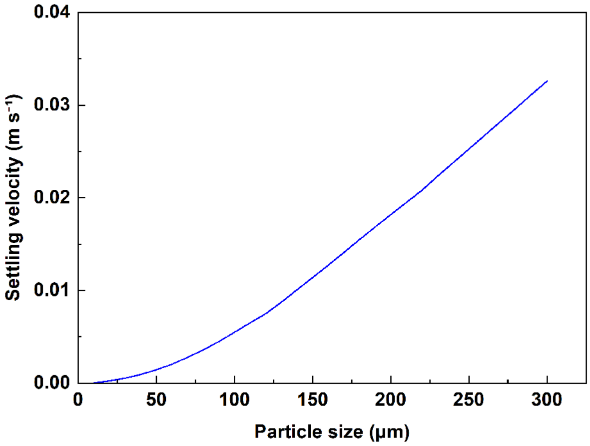

Figure 6. Effect of particle size on settling velocity

3.2.2. Experimental study

To validate the numerical results, a test was conducted to determine the required pump flow rate (Fig. 7). In the test, an acrylic tube with an inner diameter of 200 mm was employed to mimic the borehole wall and a base made of foam was installed at the bottom of the acrylic tube to simulate the borehole bottom. Notably, the foam base has an inner concave conical base that is similar as the thermal head. During testing, a simulated thermal head with an outer diameter of 180 mm was placed at the center of the acrylic tube, creating an annular space between the head and the tube for dust particle movement. The simulated thermal head has the same dimensions and shape as the real one described in Section 3.4. The tip of the simulated thermal head is equipped with two interchangeable nozzles, with diameters of 2.5 mm and 3 mm, respectively. During testing, the simulated thermal head was suspended by a forklift. Two diaphragm pumps, each with a rated flow rate of 5 L min^{-1}, were used to supply water flow. The pumps are powered by a DC power supply, and their flow rate can be adjusted by varying the input voltage from 0 to 24 V. A flowmeter and a pressure gauge were integrated into the testing system to monitor fluid resistance and flow rate. The flowmeter is a digital turbine type with a range of 0–20 L min^{-1}, a pressure rating of 0.5 MPa, and an accuracy of ± 0.5 % full scale. The pressure gauge is a digital type with a range of 0–0.6

https://doi.org/10.5194/egusphere-2026-4471
Preprint. Discussion started: 4 August 2026

MPa and an accuracy of ± 0.2 % full scale. In the experimental setup, clean water was stored at a blue water bucket, and an external red water bucket was used for collecting overflowing dust-laden water.

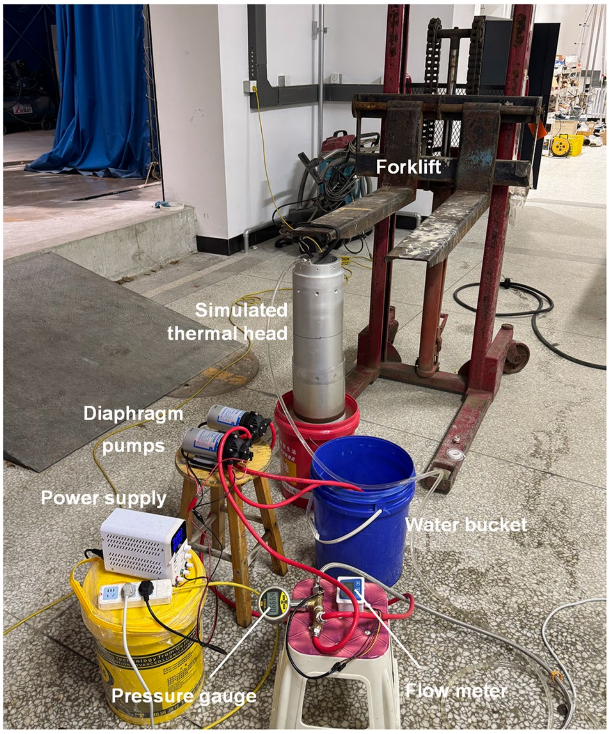

Figure 7. Experimental setup for determining required pump flow rate

220 Before testing, dust-laden water was prepared in the acrylic tube by placing commercially available river sand at the bottom of the tube. Three size fractions of dust particles were used in the tests: 50–100 μm, 100–150 μm, and 150–185 μm. In each test, 30 g of particles were uniformly distributed. Once the dust-laden water was ready, the diaphragm pumps were powered on to draw clean water from the blue water bucket and jet it through the nozzle at the tip of the simulated thermal head, washing the dust particles away from the borehole bottom. During testing, the flow rate was increased stepwise from 1.0 L min^{-1} in increments of 0.5 L min^{-1} until the dust-laden water in the acrylic tube became clear and no visible particles remained at the simulated borehole bottom (Fig. 8). This flow rate was then taken as the minimum pump flow rate required to wash away dust particles of the corresponding size. Testing results shows that the required pump flow rates for particles with size ranges of 50–100 μm, 100–150 μm, and 150–185 μm were 2.5 L min^{-1}, 6 L min^{-1}, and 9 L min^{-1}, respectively. As

https://doi.org/10.5194/egusphere-2026-4471
Preprint. Discussion started: 4 August 2026

noted earlier, dust particles in Antarctica ice sheet are typically smaller than 100 μm; therefore, a flow rate of 2.5 L min⁻¹ was determined to be sufficient for the updated RECAS thermal head. In comparison with the numerical predictions, the experimentally obtained flow rate is marginally larger.

Additional tests were performed with nozzles of 2.5 mm and 3 mm in diameter under a constant flow rate. The results indicated that nozzle diameter had no significant impact on the removing efficiency the dust particles. To obtain higher water flow velocity at borehole bottom, a nozzle with diameter of 2.5 mm was preferred to be used in updated RECAS thermal head.

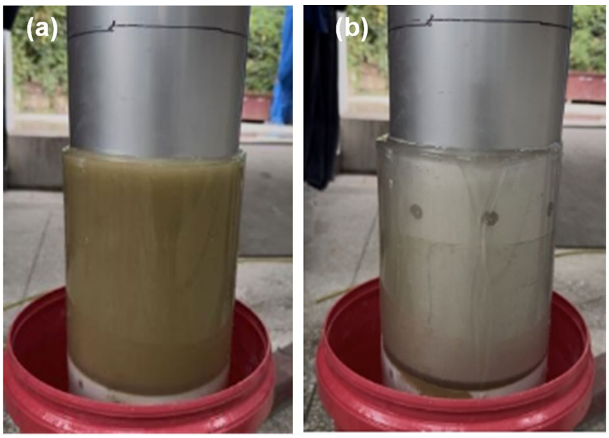

Figure 8. Visual comparison of dust-laden water: (a) before testing; (b) after testing.

3.3. Estimation of pump pressure

Due to the small nozzle diameter, inevitable pressure loss occurs during water flow. According to the study results in section 3.2, the flow rate of the built-in pump in updated RECAS thermal head is determined to be 2.5 L min^{-1}. It is necessary to estimate the pressure loss under this flow condition to determine the pump pressure.

The total pressure loss during water flow mainly consists of frictional pressure loss and local pressure loss, and can be expressed as follows

$$\Delta P = \sum \Delta P_f + \Delta P_l \quad (14)$$

https://doi.org/10.5194/egusphere-2026-4471
Preprint. Discussion started: 4 August 2026

where ΔP is the total pressure loss, Pa; ΔP_f is the frictional pressure loss, Pa; ΔP_l is the local pressure loss on filter, Pa. In our case, frictional pressure loss contains two parts, which are frictional pressure loss ΔP_{f1} in water channel inside the thermal head and the frictional pressure loss ΔP_{f2} in annulus between thermal head and ice borehole, Pa.

The Darcy–Weisbach equation is adopted to calculate the frictional pressure loss

$$\Delta P_f=\lambda\frac{L_e}{d_e}\frac{\rho {v_a}^2}{2} \quad (15)$$

where λ is the friction coefficient; L_e is the effective length of water pathway, m; d_e is the hydraulic diameter of water pathway, mm. When water flow in the channel inside the thermal head, L_e is assumed to be 1 m and d_e is assumed to be 5 mm. If borehole diameter near the thermal head is 200 mm, the hydraulic diameter in the annulus can be calculated by $d_e = D - d = 20$ mm. In our case, we can also assume that the effective length in the annulus is 1 m.

The flow velocity can be determined by following expression

$$v_a=\frac{4Q}{\pi {d_e}^2} \quad (16)$$

When water flow is turbulent, the friction coefficient can be estimated by

$$\lambda=0.3164Re^{-0.25} \quad (17)$$

where Re is Reynolds numbers and can be calculated by the following expression

$$Re = \frac{v_a d_e}{\mu} \quad (18)$$

However, when Re is <2000, the friction coefficient should be calculated by

$$\lambda = \frac{64}{Re} \quad (19)$$

The local pressure loss at the nozzle can be calculated by

$$\Delta P_l=\zeta\frac{\rho {v_a}^2}{2} \quad (20)$$

in which ζ is the local resistance coefficient. When water is discharged from a nozzle with central cylinder hole, the flow suddenly goes from a small, confined space into a very large space. In this case, the local resistance coefficient can be taken as 1.0.

https://doi.org/10.5194/egusphere-2026-4471
Preprint. Discussion started: 4 August 2026

Based on the Eq. (14) – (20), the total pressure loss can be estimated. As shown in table 2, the estimated total pressure loss is about 51639 Pa, which is quite small. Obviously, most pressure loss comes from local pressure loss at the nozzle, and frictional pressure loss in annulus between thermal head and ice borehole can be neglected. To maintain stable water flow under extreme working conditions and reserve a sufficient safety margin, the rated water head of the pump should be at least more than 10 m.

Table 2 Estimation of pressure loss

Parameter	Q (L min⁻¹)	L_e (m)	d_e (mm)	v_a (m s⁻¹)	Re	λ	ζ	ΔP (Pa)
ΔP_{f1}	2.5	1	5	2.1	7073	0.035	–	15576
ΔP_{f2}	2.5	1	20	0.007	92	0.69	–	0.84
ΔP_l	2.5	–	2.5	8.5	–	–	1	36061

3.4 Structure design

3.4.1 Overall structure design

As illustrated in Fig. 9, the updated RECAS thermal head consists of two primary components: the water circulation subsystem and the thermal melting subsystem. The former produces a water jet at the lower tip of the thermal head, whereas the latter melts ice via applied heating power. The water circulation unit is mounted directly above the thermal melting unit, and they are connected by an adapter. The adapter is provided with threads at both ends. One end is connected to the central rod of thermal melting unit, and the other end matches the central hole of the filter plate in water circulation subsystem, which is axially clamped and fixed by lock nuts. The assembly structure is compact and reliable. The updated thermal head has an overall length of 760 mm and an outer diameter of 180 mm.

https://doi.org/10.5194/egusphere-2026-4471
Preprint. Discussion started: 4 August 2026

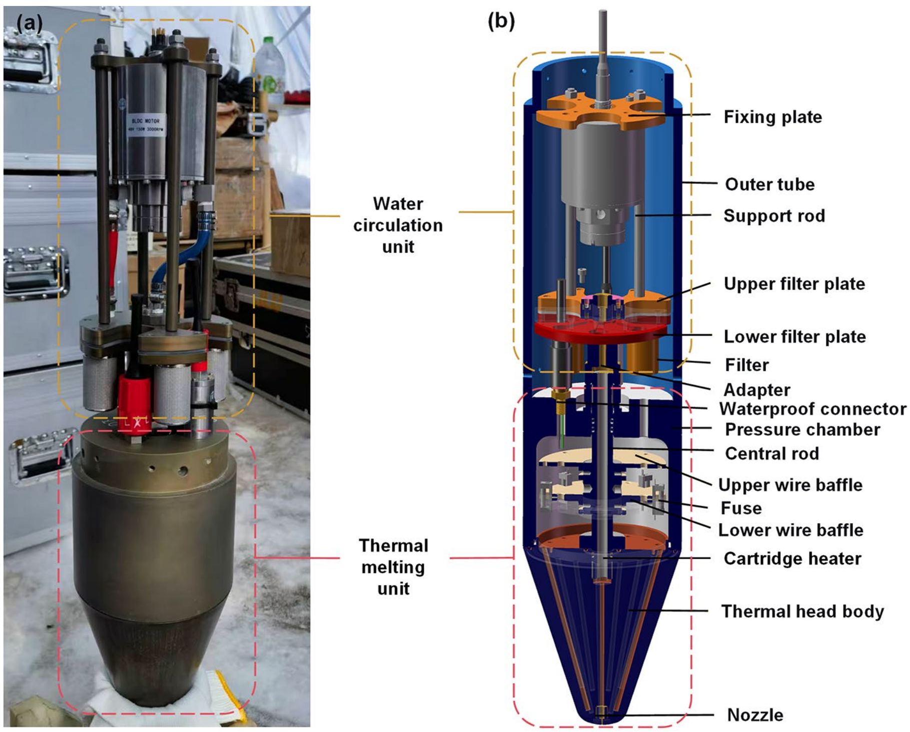

Figure 9. Updated RECAS thermal head: (a) photograph; (b) 3D model.

3.4.2 Thermal melting unit

285 The newly designed thermal melting unit has similar structure to the original RECAS thermal head (Li et al., 2020). For example, it has conical shape and was protected by pressure chamber from outer water. Nevertheless, some improvements have been made to the new thermal head.

To satisfy the 40 MPa pressure resistance specification, the present design adopts a solid structure for the thermal melting unit, with no ring groove on the thermal head body. In addition, the material of thermal head body was changed from pure 290 copper to chromium-zirconium copper, which offers greatly improved strength and comparable thermal conductivity.

The new thermal head was required to operate at high voltage of approximately 650 V. To prevent a short circuit between the neutral and live wires under high voltage conditions, two wire baffles made of polytetrafluoroethylene are added to the

https://doi.org/10.5194/egusphere-2026-4471
Preprint. Discussion started: 4 August 2026

pressure chamber to isolate the neutral wires from the live wires of cartridge heaters. Additionally, fuses are installed on the live wires to prevent voltage surges to the entire drill system in the event of a cartridge heater short circuit. Both wire baffles are fixed on the central rod, while the fuses are mounted on the lower one.

In contrast to the original RECAS thermal head, the improved design incorporates a nozzle equipped with a 2.5-mm-diameter cylindrical central hole. The nozzle is threadedly attached to the tip of the thermal head. Furthermore, a corresponding central hole is machined through both the central rod and the thermal head body.

Similar as original RECAS thermal head, the newly designed one uses cartridge heaters as heating elements. In total, 16 cartridge heaters are arranged inside the bit, including eight long cartridge heaters and eight short cartridge heaters. The long and short cartridge heaters are arranged in a staggered, symmetrical pattern and are positioned parallel to the outer surface of thermal head body. All cartridge heaters were manufactured by Hangzhou Liangdong Automation Equipment Co., Ltd., with a 10 mm cold section reserved at both the upper and lower ends. The detailed technical parameters of the cartridge heater are listed in Table 3. The 16 cartridge heaters are divided into 8 groups, each group comprising a long and a short heater connected in series, while the eight groups are wired in parallel. With a supply voltage of 650 V, the thermal head achieves a total heating power of 7040 W. Importantly, the voltage across each heater stays below the 400 V rating, which guarantees both electrical safety and operational robustness under high-voltage conditions.

Table 3. Parameters of cartridge heater

Parameter	Long cartridge heater	Short cartridge heater
Diameter (mm)	6	6
Length (mm)	200	170
Resistance (Ω)	218	263
Rated voltage (V)	400	400
Rated power (W)	734	608
Operating voltage (V)	295	355

https://doi.org/10.5194/egusphere-2026-4471
Preprint. Discussion started: 4 August 2026

Parameter	Long cartridge heater	Short cartridge heater
Operating power (W)	480	400

3.4.3 Water circulation unit

The water circulation unit mainly contains a pump and a filtration system. The pump and the filtration system are tightly fastened with the lower thermal melting unit by fixing plates, support rod, bolts and threaded connections. Additionally, an outer tube was installed above the thermal melting unit to protect the pump and the filtration system.

In the new design, the pump plays an important role in improving the drilling performance in dust-laden ice. In this study, we adopted a miniature magnetic gear pump customized by Shanghai Suofu Industrial Co., Ltd. Its main performance parameters are listed in Table 4.

Table 4. Main parameters of the magnetic gear pump

Parameter	Value
Rated voltage (V)	48 V
Rated flow rate (L min^{-1})	2.5
Rated water head (m)	30
Water pressure resistance (MPa)	40
Rated power (W)	300
Maximum diameter (mm)	80
Length (mm)	150

Given that magnetic gear pumps impose extremely high requirements on medium cleanliness during operation and consider that the thermal head may operate in dust-laden ice, a filtration system was designed at the water suction port of the pump. The filtration system comprises upper and lower filter plates, gasket, and filters, and is integrally connected to the thermal melting unit via an adapter and lock nuts. The upper and lower filter plates are fixed together by bolts, and the clearance

https://doi.org/10.5194/egusphere-2026-4471
Preprint. Discussion started: 4 August 2026

between them is sealed with a silicone gasket. Upon assembly of the upper and lower filter plates, an internal channel is created, through which the water filtered by the filters can flow. The filter is a cylinder with an outer diameter of 33 mm and a length of 85 mm. Fabricated from 400-mesh steel wire screen, it is secured to the lower filter plate by means of a threaded connection. Five such filters are employed in total, and they are alternately disposed with the waterproof connectors of the thermal melting unit to enhance space utilization. The inlet and outlet of the magnetic gear pump are connected via flexible rubber hoses. During operation, meltwater passes through the filters, enters the pump, and then flows through the adapter and the central channel of the thermal head body before being discharged from the nozzle.

4 Test of the updated RECAS thermal head

4.1 Water pressure resistance test

Water pressure resistance tests of the magnetic gear pump and the thermal melting unit were conducted independently in a high-pressure chamber. During testing, the water pressure in the high-pressure chamber gradually increased to 40 MPa at a rate of 2 MPa min^{-1}. It was then held at this pressure for about 1 h, after which it was gradually reduced to 0 MPa at the same rate (Fig. 10). Notably, when the pressure in the high-pressure chamber reached 40 MPa, the magnetic gear pump was activated with no load, and its status was checked by monitoring the operating current. It was confirmed that the pump can operate stably in 40 MPa water, drawing an input current of 0.6 A. After testing, the magnetic gear pump and thermal melting unit were extracted from the chamber, and no structural deformation or water leakage was observed. The test results demonstrate that both the thermal melting unit and the magnetic gear pump function properly under a water pressure of 40 MPa.

https://doi.org/10.5194/egusphere-2026-4471
Preprint. Discussion started: 4 August 2026

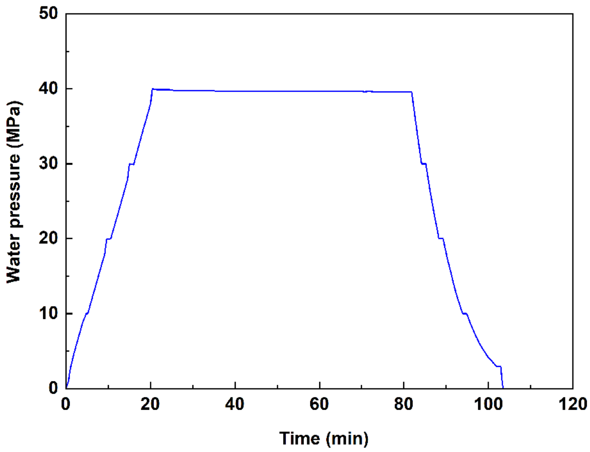

340 **Figure 10. Water pressure resistance test of the magnetic gear pump and the thermal melting unit**

4.2 Drilling performance in clean ice

The updated RECAS thermal head was first tested in clean ice. As shown in Fig. 11, the test was conducted on the same test stand used previously (Talalay et al., 2019; Li et al., 2020). Notably, in the test, the original transformer was replaced by a larger one with maximum input voltage of 1000 V. Furthermore, a bucket served as the water storage container. The clean ice samples were fabricated in a freezing container at −20 °C. During fabrication, tap water was frozen layer by layer in a 1 m iron barrel. This method prevents freezing-induced deformation and produces uniformly clear ice with no bubbles or cracks.

https://doi.org/10.5194/egusphere-2026-4471
Preprint. Discussion started: 4 August 2026

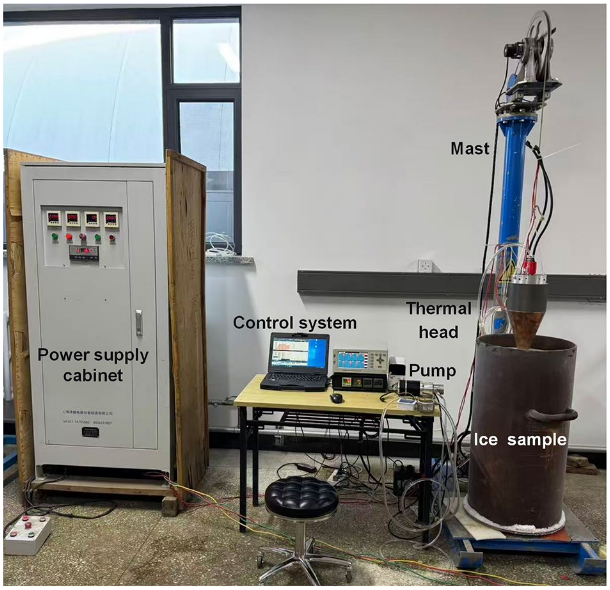

Figure 11. Test stand of the updated RECAS thermal head

In the test, the heating power of the thermal head was set to 7000 W, and the weight on thermal head was stabilized at approximately 150 N. The magnetic gear pump was operated at its rated flow rate of 2.5 L min^{-1}. The test process can be divided into two stages. In the first stage, the magnetic gear pump was deactivated, and the ice was penetrated solely by the thermal melting drilling method, hereafter referred to as TMD. During the second stage, the magnetic gear pump was turned on to extract borehole water and discharge it through the nozzle. The drilling process thus combines TMD with meltwater jetting. Herein, this method is designated as thermal melting drilling with water jetting (TMDWJ).

As shown in Fig. 12a, the thermal head drilled about 0.15 m in ice with the method of TMD and then changed to drill by TMDWJ method until the drilling depth reached about 0.5 m. The results show that the average ROP in TMD mode was 1.74 m h^{-1} (Fig. 12b). After meltwater injection was enabled, the average ROP increased to 2.12 m h^{-1}, indicating that water circulation enhanced heat transfer between the thermal head and the surrounding ice, leading to an increase of approximately 21.8 % in ROP. During the entire drilling process, the meltwater temperature in the borehole remained between 2.5 and 5 °C, with an average of 3.5°C. After testing, the borehole diameter was measured at approximately 200 mm. Overall, these results confirm that meltwater jetting can effectively improve the ROP in clean ice.

https://doi.org/10.5194/egusphere-2026-4471
Preprint. Discussion started: 4 August 2026

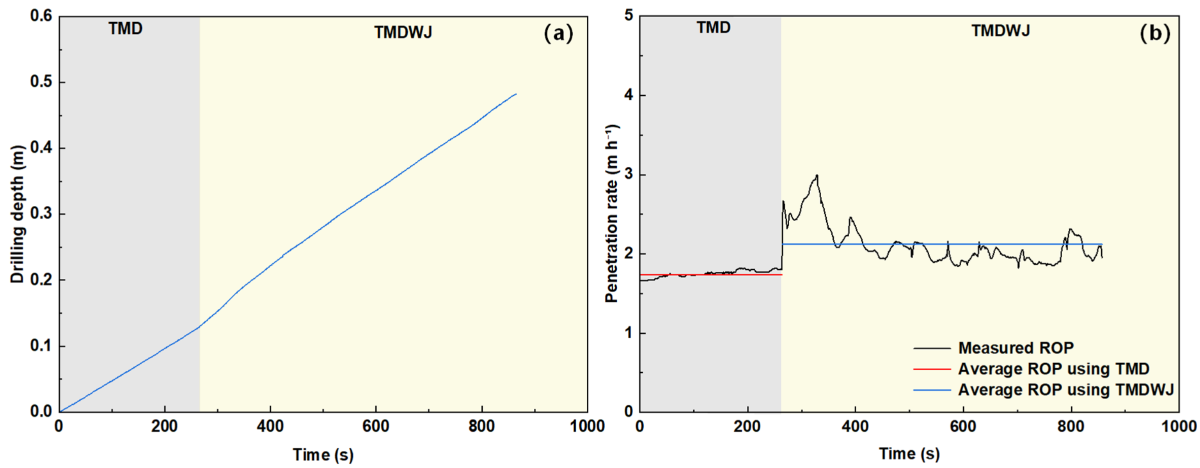

Figure 12. Variation of: (a) drilling depth; and (b) ROP with time during drilling in clean ice.

4.3 Drilling performance in dust-laden ice

Dust-laden ice samples were prepared following the procedure described by Li et al. (2020). In preparation, dust particles with a minimum size of 250 μm were selected to ensure conservative and reliable test conditions, as this size exceeds the typical particle sizes found in Antarctic ice sheet. The dust-laden ice layer was prepared with a thickness of approximately 2 cm and was positioned about 30 cm below the ice surface. The dust-laden ice sample was frozen at −15 °C. To ensure comparability of the experimental results, the operational parameters were kept consistent with those used in the clean ice tests. Specifically, the weight on thermal head stabilized at 150 N, and the heating power was set to 7 kW. The same as mentioned in section 4.2, both the TMD and the TMDWJ methods were used for ice drilling. When drilling in TMDWJ methods, the flow rate of the magnetic gear pump remained at 2.5 L min^{-1}.

In the test, the borehole was first deepened to 0.2 m using TMD and then drilled to 0.7 m using the TMDWJ method (Fig. 12a). Notably, in Fig. 13, time zero corresponds to the moment when the thermal head reaches the dust-laden ice layer. As shown in Fig. 13b, the average ROP in dust-laden ice is 1.46 m h^{-1}, which was 16.1 % lower than that in clean ice. Benefiting from the scouring effect of circulating meltwater, the TMDWJ method can effectively remove dust attached to the thermal head surface and enhance heat transfer between the thermal head and the ice. Consequently, the average ROP increased to

https://doi.org/10.5194/egusphere-2026-4471
Preprint. Discussion started: 4 August 2026

2.06 m·h⁻¹, which is nearly identical to that observed in clean ice. Overall, the TMDWJ method achieved a 41.1 % increase in ROP when applied to dust-laden ice drilling. After drilling, the borehole diameter was measured to be 217 mm in the upper part and 203 mm in the lower part.

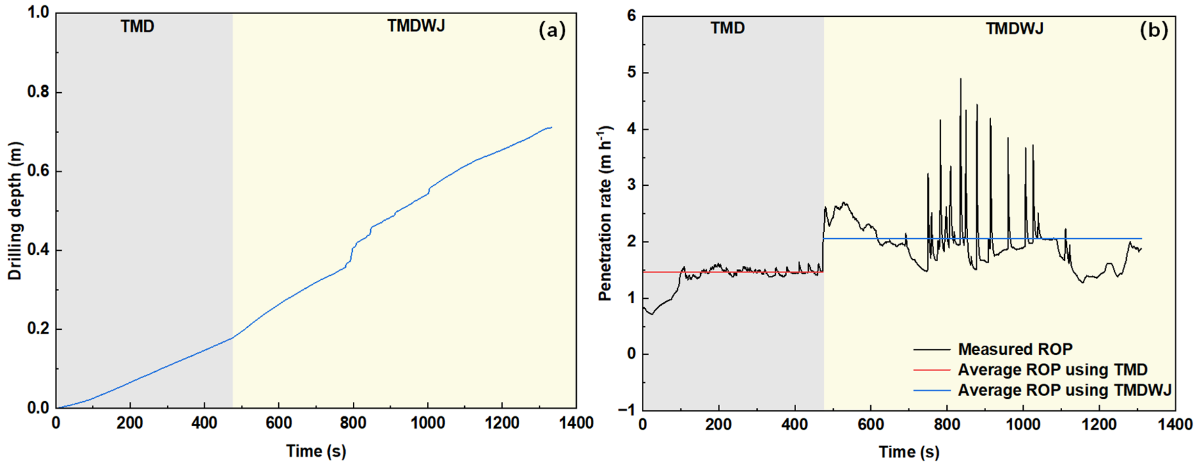

Figure 13. Variation of: (a) drilling depth; and (b) ROP with time during drilling in dust-laden ice.

4.4 Drilling performance in debris-rich ice

In addition to fine ash particles, Antarctic ice may also contain rock clasts, which severely reduce ROP of thermal head. To simulate such extreme conditions, test was carried out on debris-rich ice. Before testing, ice samples were prepared using tap water in the same barrels as in previous tests. During preparation, each barrel was first filled with tap water to 50 % of its volume and frozen at −15 °C for 24 h to form a dense ice layer. Five pebbles with diameter of 0.5–1.5 cm were then evenly placed at the center of this ice layer. Finally, tap water was slowly added to reach 80 % volume to avoid displacing the pebbles, followed by continuous freezing for 48 h to ensure firm bonding between the pebbles and the ice.

In the test, the weight on thermal head and the heating power remained consistent with previous tests. The whole test was divided into four stages. In the first stage, the thermal head was used to drill clean ice using the TMD method. In the second stage, the thermal head continued drilling in debris-rich ice with the same method. In the third stage, the thermal head was lifted slightly to allow trapped pebbles to fall to the borehole bottom, and then it was reinserted into the hole. This stage is

https://doi.org/10.5194/egusphere-2026-4471
Preprint. Discussion started: 4 August 2026

referred to as "tripping". In the final stage, the magnetic gear pump was activated to resume drilling with the TMDWJ method.

As shown in Fig. 14, the testing results show that the ROP of the thermal head remained at about 1.98 m h^{-1} in clean ice. When the thermal head contacted hard pebbles, the ROP suddenly dropped to nearly zero. However, continued heating of the thermal head warmed the water beneath it, leading to slow melting of the underlying ice. This gave a ROP of 0.65 m h^{-1}, which was only 33.3 % of that observed in clean ice. After thermal head was lifted and the magnetic gear pump was activated, the average ROP in last drilling stage recovered to 2.05 m h^{-1}, which is comparable to the performance in clean ice.

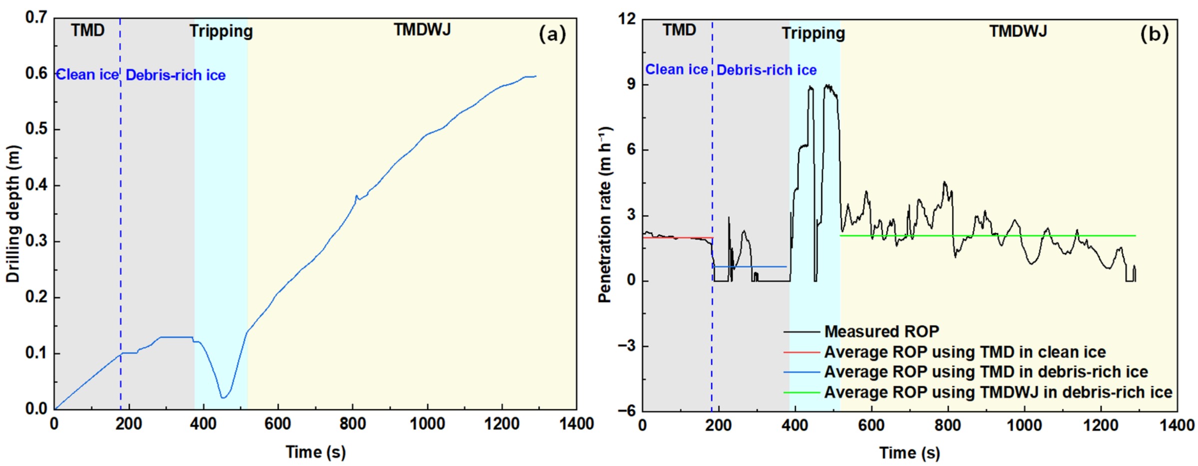

Figure 14. Variation of: (a) drilling depth; and (b) ROP with time during drilling in debris-rich ice.

After drilling, the meltwater in the borehole was drained, and the borehole morphology was replicated using polyurethane foam. Further inspection of the borehole morphology indicates that the jetting meltwater formed a local enlarged cavity beneath the tip of the thermal head. This cavity is believed to have provided accommodation space for fallen pebbles, thereby preventing persistent blockage of the melting interface by pebbles. This explains why the ROP recovered after the TMDWJ method was applied in debris-rich ice. In conclusion, the combined strategy of periodic lifting and meltwater jetting enables the thermal head to drill efficiently in debris-rich ice containing rock clasts.

https://doi.org/10.5194/egusphere-2026-4471
Preprint. Discussion started: 4 August 2026

5 Conclusions

In this study, the original RECAS thermal head was redesigned and tested to improve its pressure resistance and drilling performance in dust-laden and debris-rich ice. The main conclusions are as follows.

(1) A water circulation unit, consisting mainly of a magnetic gear pump and a filtration system, was added above the original RECAS thermal head to achieve better drilling performance in dust-laden ice and debris-rich ice. The updated RECAS thermal head has an overall length of 760 mm and an outer diameter of 180 mm. To achieve a ROP of no less than 2 $m \cdot h^{-1}$, the newly developed thermal head was designed with a heating power of 7000 W at 650 V.

(2) To maintain suspension and upward transport of dust particles smaller than 100 μm, the rated flow rate of the magnetic gear pump was determined to be 2.5 $L \cdot min^{-1}$. Theoretical calculations further indicate that the pump head should be no less than 10 m to compensate for pressure losses in the circulation loop.

(3) Experimental results verified that the magnetic gear pump could operate stably under a water pressure of 40 MPa. In addition, the updated thermal head was also capable of withstanding such high pressure, achieved by replacing the head material from pure copper to chromium-zirconium copper and adopting a solid construction.

(4) The TMDWJ method improved the ROP compared with the TMD method. In clean ice, the ROP reached 2.12 m h^{-1} with the water circulation system activated, which is 21.8 % higher than that of thermal melting drilling. In dust-laden ice, the ROP was 2.06 m h^{-1} using TMDWJ method, representing an efficiency improvement of 41.1 %. In debris-rich ice, the ROP could recover to 2.05 m h^{-1} from 0.65 m h^{-1} by combining intermittent tripping and meltwater circulation.

Overall, the updated RECAS thermal head can operate under a water pressure of 40 MPa and achieve improved drilling performance in complex ice layers, such as dust-laden ice and debris-rich ice. It is expected to be deployed to drill Qilin Subglacial Lake during the 2026–2027 Antarctic season.

Data availability

All raw data used in this article can be found in the Supplement.

https://doi.org/10.5194/egusphere-2026-4471
Preprint. Discussion started: 4 August 2026

Author contribution

FX designed the project and provided financial support.; LY designed the new thermal head with the contribution from LX FX, LB and YY; YH and PS performed water pressure resistance test; LY, LX carried out drilling test in ice; LY prepared the manuscript with contributions from all co-authors.

Competing interests

The contact author has declared that none of the authors has any competing interests.

Acknowledgement

We thank graduate students Xinlong Che and Shibo Zhang from China University of Geosciences, Beijing, for their help in conducting the tests, and we also thank graduate students Xu Zhang and Ximu Liu from Jilin University for their assistance in preparing the ice samples and testing equipment.

Financial support

This research has been supported by the National Key Research and Development Project of the Ministry of Science and Technology of China [grant numbers 2023YFC2812602 and 2021YFC2801403]; the Fundamental and Interdisciplinary Disciplines Breakthrough Plan of the Ministry of Education of China [grant number JYB2025XDXM803].

References

Bulat, S. A.: Microbiology of the subglacial Lake Vostok: first results of borehole-frozen lake water analysis and prospects for searching for lake inhabitants, Philos. Trans. R. Soc. A, 374, 20140292, https://doi.org/10.1098/rsta.2014.0292, 2016.

https://doi.org/10.5194/egusphere-2026-4471
Preprint. Discussion started: 4 August 2026

Christner, B. C., Priscu, J. C., Achberger, A. M., Barbante, C., Carter, S. P., Christianson, K., Michaud, A. B., Mikucki, J. A., Mitchell, A. C., Skidmore, M. L. and Vick-Majors, T. J. and the WISSARD Science Team: A microbial ecosystem beneath the West Antarctic ice sheet, Nature, 512, 310–313, https://doi.org/10.1038/nature13667, 2014.

Cuffey, K. M. and Paterson, W. S. B. (Eds.): The physics of glaciers, (fourth edition), Butterworth-Heinemann/Elsevier, Burlington, MA, USA, 693 pp., ISBN 9780123694614, 2010.

Dachwald, B., Mikucki, J., Tulaczyk, S., Digel, I., Espe, C., Feldmann, M., Francke, G., Kowalski, J. and Xu, C.: IceMole: a maneuverable probe for clean in situ analysis and sampling of subsurface ice and subglacial aquatic ecosystems, Ann. Glaciol., 55, 14–22, https://doi.org/10.3189/2014AoG65A004, 2014.

Delmonte, B., Petit, J. R. and Maggi, V.: LGM-Holocene changes and Holocene millennial-scale oscillations of dust particles in the EPICA Dome C ice core, East Antarctica, Ann. Glaciol., 35, 306–312, https://doi.org/10.3189/172756402781816843, 2002.

Eppelbaum, L.V. and Kutasov, I.M.: Well drilling in permafrost regions – dynamics of the thawed zone, Polar Research, 38, 1-9, https://doi.org/10.33265/polar.v38.3351, 2019.

Fretwell, P., Pritchard, H. D., Vaughan, D. G., Bamber, J. L., Barrand, N. E., Bell, R., Bianchi, C., Bingham, R. G., Blankenship, D. D., Casassa, G., Catania, G., Callens, D., Conway, H., Cook, A. J., Corr, H. F. J., Damaske, D., Damm, V., Ferraccioli, F., Forsberg, R., Fujita, S., Gim, Y., Gogineni, P., Griggs, J. A., Hindmarsh, R. C. A., Holmlund, P., Holt, J. W., Jacobel, R. W., Jenkins, A., Jokat, W., Jordan, T., King, E. C., Kohler, J., Krabill, W., Riger-Kusk, M., Langley, K. A., Leitchenkov, G., Leuschen, C., Luyendyk, B. P., Matsuoka, K., Mouginot, J., Nitsche, F. O., Nogi, Y., Nost, O. A., Popov, S. V., Rignot, E., Rippin, D. M., Rivera, A., Roberts, J., Ross, N., Siegert, M. J., Smith, A. M., Steinhage, D., Studinger, M., Sun, B., Tinto, B. K., Welch, B. C., Wilson, D., Young, D. A., Xiangbin, C. and Zirizzotti, A.: Bedmap2: improved ice bed, surface and thickness datasets for Antarctica, Cryosphere, 7, 375–393, https://doi.org/1.5194/tc-7-375-2013, 2013.

Gillet, F.: Steam, hot-water and electrical thermal drills for temperate glaciers, J. Glaciol., 14, 171–179, https://doi.org/10.3189/S0022143000013484, 1975.

https://doi.org/10.5194/egusphere-2026-4471
Preprint. Discussion started: 4 August 2026

Hantz, D. and Lliboutry, L.: Waterways, ice permeability at depth, and water pressures at Glacier d'Argentière, French Alps, J. Glaciol., 29, 227–239, https://doi.org/10.3189/S0022143000008285, 1983.

Heinen, D., Audehm, J., Becker, F., Boeck, G., Espe, C., Feldmann, M., Francke, G., Friend, P., Haberberger, N., Helbing, K., Nghe, C.T., Stelzig, M., Vossiek, M., Wiebusch, C., Zierke, S.: The TRIPLE melting probe - an electro-thermal drill with a forefield reconnaissance system to access subglacial lakes and oceans, in: OCEANS 2021, San Diego, CA, USA., 20-23 September 2021, 1–7, https://doi.org/10.23919/OCEANS44145.2021.9705999, 2021.

Kohno, M., Fujii, Y. and Hirata, T.: Chemical composition of volcanic glasses in visible tephra layers found in a 2503 m deep ice core from Dome Fuji, Antarctica, Ann. Glaciol., 39, 576–584, https://doi.org/10.3189/172756404781813934, 2004.

Kutasov, I. M. and Eppelbaum, L. V.: The effect of thermal properties changing (at ice-water transition) on the radius of permafrost thawing, Cold Reg. Sci. Technol., 151, 156–158, https://doi.org/10.1016/j.coldregions.2018.03.018, 2018.

Leitchenkov, G. L., Antonov, A. V., Luneov, P. I. and Lipenkov, V. Y.: Geology and environments of subglacial Lake Vostok, Philos. Trans. R. Soc. A, 374, 20140302, https://doi.org/10.1098/rsta.2014.0302, 2016.

Leitchenkov, G. L., Belyatsky, B. V., Rodionov, N. V. and Sergeev, S. A.: Insight into the geology of the East Antarctic hinterland: a study of sediment inclusions from ice cores of the Lake Vostok borehole, U.S. Geol. Surv. Open-File Rep., 2007-1047-SRP-014, https://doi.org/10.3133/ofr20071047SRP014, 2007.

Li, Y., Liu, L., Fan, X., Li, B., Zhang, N., Gong, D., Lei, X.: Numerical simulation of borehole closure process by freezing during drilling into Qilin Subglacial Lake, Sci. Technol. Eng., 26, 4148–4157, https://doi.org/10.12404/j.issn.1671-1815.2503018, 2026. (Text in Chinese)

Li, Y., Talalay, P. G., Sysoev, M. A., Zagorodnov, V. S., Li, X. and Fan, X.: Thermal heads for melt drilling to subglacial lakes: design and testing, Astrobiology, 20, 142–156, https://doi.org/10.1089/ast.2019.2103, 2020.

Li, Z., Cui, X., Xu, B., Hu, K., Li, D., Li, L., Guo, J., Chen, Y. and Sun, B.: Basal melt rate over the Subglacial Lake Qilin derived through an optimized 1–D steady–state thermodynamic model, N. Z. J. Geol. Geophys., 69, e70049, https://doi.org/10.1002/jgo2.70049, 2026.

Livingstone, S. J., Li, Y., Rutishauser, A., Sanderson, R. J., Winter, K., Mikucki, J. A., Björnsson, H., Bowling, J. S., Chu, W., Dow, C. F., Fricker, H. A., McMillan, M., Ng, F. S. L., Ross, N., Siegert, M. J., Siegfried, M. and Sole, A. J.: Subglacial lakes and their changing role in a warming climate, Nat. Rev. Earth Environ., 3, 106–124, https://doi.org/10.1038/s43017-021-00246-9, 2022.

Lu, K. and Chen, Y.: Active-source seismic characterization of subglacial lakes: numerical modeling, field validation, and implications for Antarctic exploration, Cryosphere, 20, 1497–1522, https://doi.org/10.5194/tc-20-1497-2026, 2026.

Narcisi, B., Petit, J.R. and Langone, A.: Last glacial tephra layers in the Talos Dome ice core (peripheral East Antarctic Plateau), with implications for chronostratigraphic correlations and regional volcanic history, Quat. Sci. Rev., 165, 111, https://doi.org/10.1016/j.quascirev.2017.04.025, 2017.

Oswald, G. K. A. and Robin, G. de Q.: Lakes beneath the Antarctic Ice Sheet, Nature, 245, 251–254, https://doi.org/10.1038/245251a0, 1973.

Priscu, J. C., Adams, E. E., Lyons, W. B., Voytek, M. A., Mogk, D. W., Brown, R. L., McKay, C. P., Takacs, C. D., Welch, K. A., Wolf, C. F., Kirshtein, J. D. and Avci, R.: Geomicrobiology of subglacial ice above Lake Vostok, Antarctica, Science, 286, 2141–2144, https://doi.org/10.1126/science.286.5447.2141, 1999.

Priscu, J.C., Kalin, J., Winans, J., Campbell, T., Siegfried, M.R., Skidmore, M., Dore, J.E., Leventer, A., Harwood, D.M., Duling, D., Zook, R., Burnett, J., Gibson, D., Krula, E., Mironov, A., McManis, J., Roberts, G., Rosenheim, B.E., Christner, B.C., Kasic, K., Fricker, H.A., Lyons, W.B., Barker, J., Bowling, M., Collins, B., Davis, C., Gagnon, A., Gardner, C., Gustafson, C., Kim, O.-S., Li, W., Michaud, A., Patterson, M.O., Tranter, M., Venturelli, R., Vick-Majors, T. and Elsworth, C. and the SALSA Science Team: Scientific access into Mercer Subglacial Lake: scientific objectives, drilling operations and initial observations, Ann. Glaciol., 62, 340–352, https://doi.org/10.1017/aog.2021.10, 2021.

Robin, G. de Q., Swithinbank, C. W. M. and Smith, B. M. E.: Radio echo exploration of the Antarctic ice sheet, in: International Symposium on Antarctic Glaciological Exploration (ISAGE), Hanover, New Hampshire, USA, 3-7 September 1968. 97-115,1970.

https://doi.org/10.5194/egusphere-2026-4471
Preprint. Discussion started: 4 August 2026

Schüller, K., Kowalski, J., and Råback, P.: Curvilinear melting – A preliminary experimental and numerical study, Int. J. Heat Mass Transf., 92, 884-892, https://doi.org/10.1016/j.ijheatmasstransfer.2015.09.046, 2016.

Siegert, M. J.: Antarctic subglacial lakes, Earth-Sci. Rev., 50, 29–50, https://doi.org/10.1016/s0012-8252(99)00068-9, 2000.

Siegert, M. J., Clarke, R. J., Mowlem, M., Ross, N., Hill, C. S., Tait, A., Hodgson, D., Parnell, J., Tranter, M., Pearce, D., Bentley, M. J., Cockell, C., Tsaloglou, M.-N., Smith, A., Woodward, J., Brito, M. P. and Waugh, E.: Clean access, measurement, and sampling of Ellsworth Subglacial Lake: A method for exploring deep Antarctic subglacial lake environments, Rev. Geophys., 50, RG1003, https://doi.org/10.1029/2011RG000361, 2012.

Siegert, M. J., Makinson, K., Blake, D., Mowlem, M. and Ross, N.: An assessment of deep hot-water drilling as a means to undertake direct measurement and sampling of Antarctic subglacial lakes: experience and lessons learned from the Lake Ellsworth field season 2012/13, Ann. Glaciol., 55, 59–73, https://doi.org/10.3189/2014AoG65A008, 2014.

Stone, W. C., Hogan, B.P., Siegel, V., Lelievre, S. and Flesher, C.: Progress towards an optically powered cryobot, Ann. Glaciol., 55, 1–11, https://doi.org/10.3189/2014AoG65A200, 2014.

Stone, W. C., Hogan, B., Siegel, V., Harman, J., Flesher, C., Clark, E., Pradhan, O., Gasiewski, A., Howe, S. and Howe, T.: Project VALKYRIE: laser-powered cryobots and other methods for penetrating deep ice on ocean worlds, in: Outer Solar System: Prospective Energy and Material Resources, edited by: Badescu, V. and Zacny, K., Springer, Cham, Switzerland, 47–165, https://doi.org/10.1007/978-3-319-73845-1_4, 2018.

Sun, Y., Talalay, P. G., Li, Y., Yu, H., Wang, D., Li, G., Xu, L., Gong, D., Wang, J., Wang, J., Wang, T., Zhang, N., Wang, Z., Chen, Y., Liu, Y., Li, Y., Peng, S., Shi, J., An, C., Ge, Q., Xu, J., Ni, X., Cui, Q., Jiang, Q., Sysoev, M. A., Yang, Y., Wang, R., Wei, X., Wang, Y., Zhu, T., Deng, Z., Markov, A., Li, B. and Fan, X.: Exploring Antarctic subglacial lakes with RECoverable Autonomous Sonde (RECAS): Design and first field tests, Sci. China Technol. Sci., 67, 1866–1878, https://doi.org/10.1007/s11431-023-2620-3, 2024.

Sysoev, M. A., Talalay, P. G., Fan, X., Zhang, N., Gong, D., Yang, Y., Wang, T., and Deng, Z.: A steerable system for the RECoverable Autonomous Sonde (RECAS) to access and study subglacial lakes, Geosci. Instrum. Method. Data Syst., 14, 29–43, https://doi.org/10.5194/gi-14-29-2025, 2025.

https://doi.org/10.5194/egusphere-2026-4471
Preprint. Discussion started: 4 August 2026

Talalay, P. G., Li, Y., Sysoev, M. A., Hong, J., Li, X. and Fan, X.: Thermal tips for ice hot-point drilling: Experiments and preliminary thermal modeling, Cold Reg. Sci. Technol., 160, 97–109, https://doi.org/10.1016/j.coldregions.2019.01.015, 2019.

Talalay, P. G., Zagorodnov, V. S., Markov, A. N., Sysoev, M. A. and Hong J.: Recoverable autonomous sonde (RECAS) for environmental exploration of Antarctic subglacial lakes: general concept, Ann. Glaciol., 55, 23–30, https://doi.org/10.3189/2014AoG65A003, 2014.

Tsytovich, N. A. (Eds.): The mechanics of frozen ground, Scripta Book Co., Washington, DC, USA, 426pp., 1975.

Wirtz, M. and Hildebrandt, M.: IceShuttle Teredo: an ice-penetrating robotic system to transport an exploration AUV into the ocean of Jupiter's moon Europa, in: 67th International Astronautical Congress (IAC), Guadalajara, Jalisco, Mexico, 26–30 September 2016, 1–11, 2016.

Yan, S., Blankenship, D. D., Greenbaum, J. S., Young, D. A., Li, L., Rutishauser, A., Guo, J., Roberts, J. L., van Ommen, T. D., Siegert, M. J. and Sun, B.: A newly discovered subglacial lake in East Antarctica likely hosts a valuable sedimentary record of ice and climate change, Geology, 50, 949–953, https://doi.org/10.1130/G50009.1, 2022.

Yan, S., Koutnik, M. R., Blankenship, D. D., Greenbaum, J. S., Young, D. A., Roberts, J. L., van Ommen, T., Sun, B. and Siegert, M. J.: Holocene hydrological evolution of subglacial Lake Snow Eagle, East Antarctica, implied by englacial radio stratigraphy, J. Glaciol., 71, e29, 1–15, https://doi.org/10.1017/jog.2025.15, 2025.

Zhao, G., Talalay, P. G., Fan, X., Zhang, N., Liu, Y., Wang, T. and Chen, Y.: Optimization of hot-water drilling in ice with near-bottom circulation, Water, 14, 127, https://doi.org/10.3390/w14010127, 2022.

Zhou, Y., Cui, X., Dai, Z., Zhou, X., Li, L., Jiang, S. and Sun, B.: The Antarctic subglacial hydrological environment and international drilling projects: a review, Water, 16, 1111, https://doi.org/10.3390/w16081111, 2024.

Zimmerman, W., Anderson, F., Carsey, F., Conrad, P., Englehardt, H., French, L. and Hecht, M. The Mars '07 North Polar Cap deep penetration cryo-scout mission, in: 2002 IEEE Aerospace Conference Proceedings, Big Sky, MT, USA, 09-16 March 2002, 305–315, https://doi.org/10.1109/AERO.2002.1036850, 2002.

https://doi.org/10.5194/egusphere-2026-4471
Preprint. Discussion started: 4 August 2026

565 Zimmerman, W., Bonitz, R. and Feldman, J.: Cryobot: an ice penetrating robotic vehicle for Mars and Europa, in: 2001 IEEE Aerospace Conference Proceedings, Big Sky, MT, USA, 10-17 March 2001, 311–323, https://doi.org/10.1109/AERO.2001.931722, 2001.